イオン蓄積・冷却リングS-LSRでのMGイオンビームのレーザー冷却

野田 章[A)], 中尾 政夫[A)], 想田 光[B)], 頓宮 拓[C)],
岡本 宏巳[D)], 大崎 一哉[D)], 百合 庸介[E)]、神保 光一[F)],
グリーザー マンフレッド[G)]、何 崢麒[H)]

[A)]NIRS, [B)]Gunma Univ. [C)]ICR, Kyoto Univ.
[D)] AdSM, HiroshimaUniv., [E)]JAEA, TARRI., [F)]IAE, Kyoto Univ.
[G)]MPI-K,, Germany, [H)] Tsinghua Univ., China

Contents

1. 先進小型加速器のための要素技術開発
2. S-LSRの概要
3. SBRCによる間接的横方向レーザー冷却
4. スクレーパーを用いたビーム強度制御によるIBS抑制と冷却効率の改善
5. 現在までの到達点

Development of Compact Cancer Therapy Machine with Use of Laser Ion Source

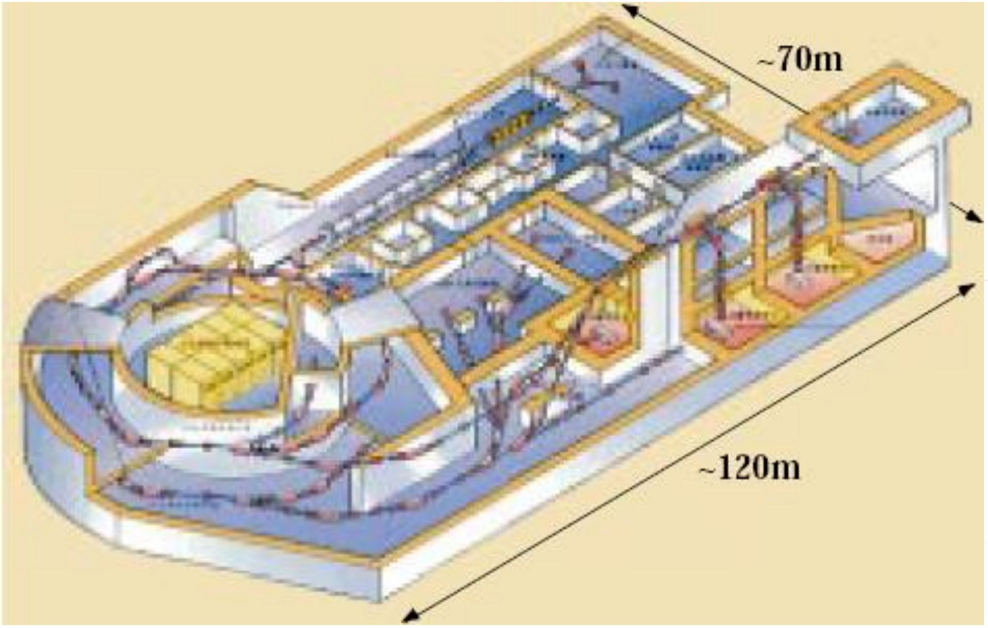

HIMAC at NIRS in Chiba

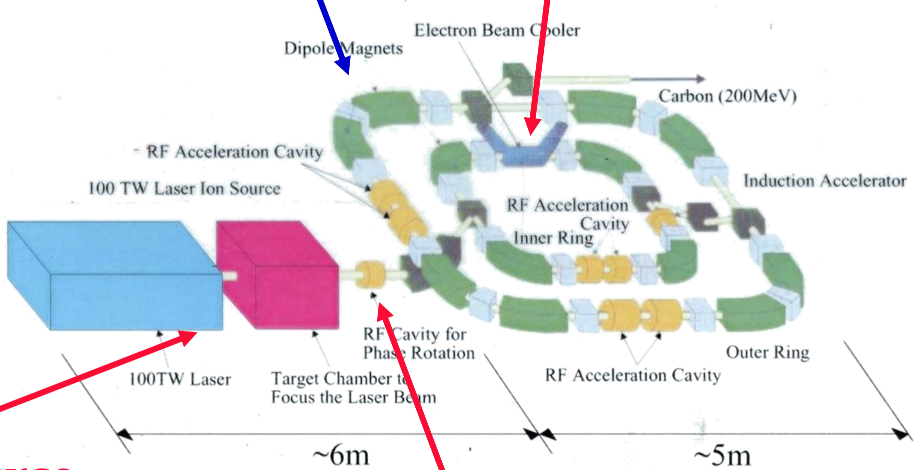

Compact Heavy-Ion (Carbon Ion) Synchrotron

Compact Cooler Ring S-LSR

ー Circumference 22.56m
ー Straight Section Length 1.86m

E-cooling modes

- Protons 7MeV (Ee=3.8keV)

Laser cooling

- $^{24}Mg^{+}$ 40 keV
  (l=282 nm)

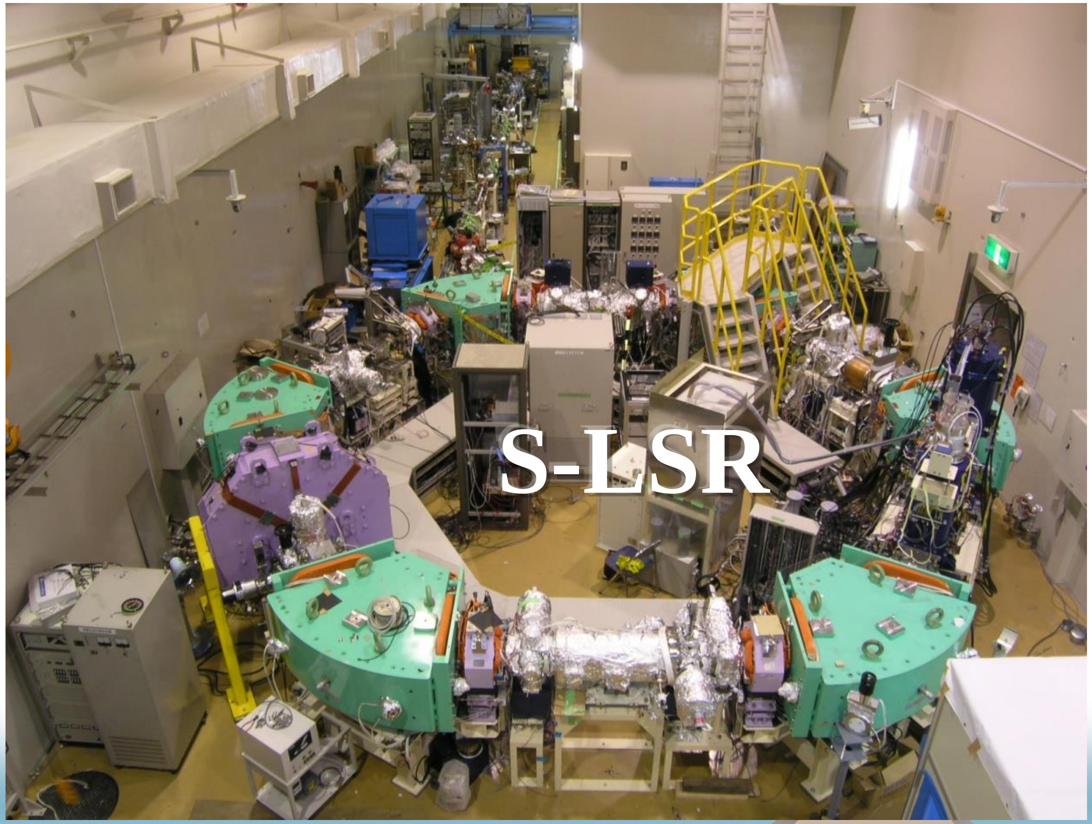

In operation since October, 2005

Main Parameters of S-LSR

Circumference	22.557 m
Average radius	3.59 m
Length of straight section	1.86 m
Number of periods	6
Betatron Tune	
Crystalline Mode	Normal Operation Mode
1.45 (H) , 1.44 (V)	1.872(H), 0.788 (V): EC
	2.068(H), 1.105, 1.070 (V): LC
Bending Magnet	(H-type)
Maximum field	0.95 T
Curvature radius	1.05 m
Gap height	70 mm
Pole end cut	Rogowski cut+Field clamp
Deflection Angle	60°
Weight	4.5 tons
Quadrupole Magnet	
Core Length	0.20 m
Bore radius	70 mm
Maximum field gradient	5 T/m

ESR at GSI, by M. Steck

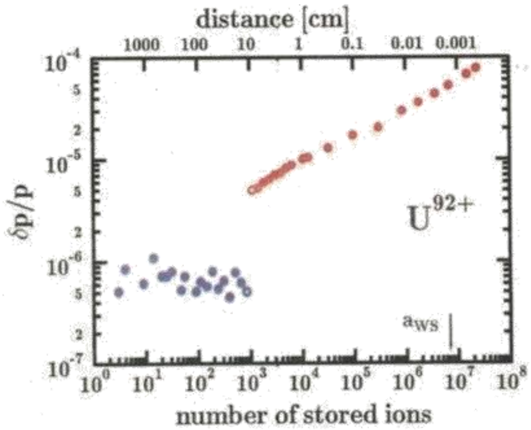

Figure 2. Experimental momentum spreads from Schottky signals vs. number of stored ions in the ESR for electron cooled U^{92+} ions at 240 MeV/u. a_{WS} indicates the Wigner-Seitz radius of eq.(3). (after ref. [9])

CRYRING at Stockholm, by H. Danared

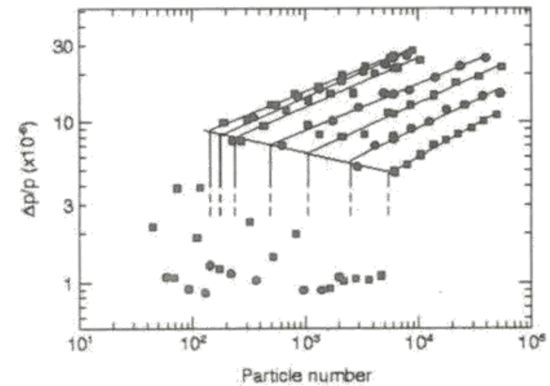

Fig. 5: Relative momentum spread as a function of particle number for the lowest seven electron densities represented in Fig. 2. The density increases from the upper left to the lower right. For each density, a line is fitted to the data points. A line is also drawn through the points corresponding to the transition to the ordered state. (The use of different symbols is just to help identifying which points belong to same electron density.)

ESR at GSI, by M. Steck

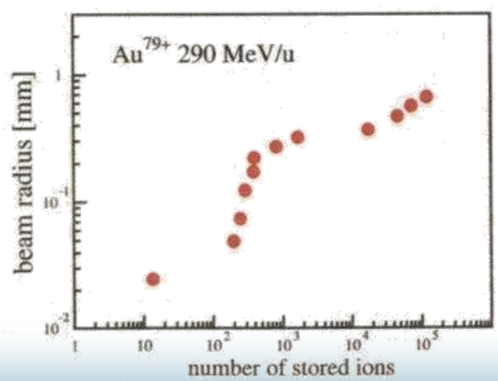

Figure 3. Beam radius measured with a beam scraper vs. number of stored ions in the ESR for electron cooled Au^{79+} ions at 290 MeV/u (from ref. [10]).

NAP-M at BINP, Novosibirsk by V.V. Parkhomchuk

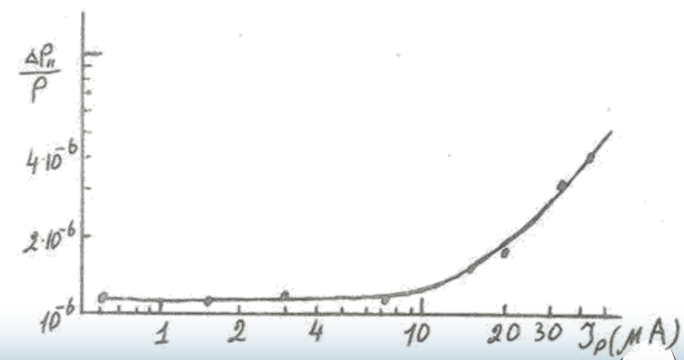

Fig. 6. The momentum spread of proton beam versus current J_p.

Ring Layout

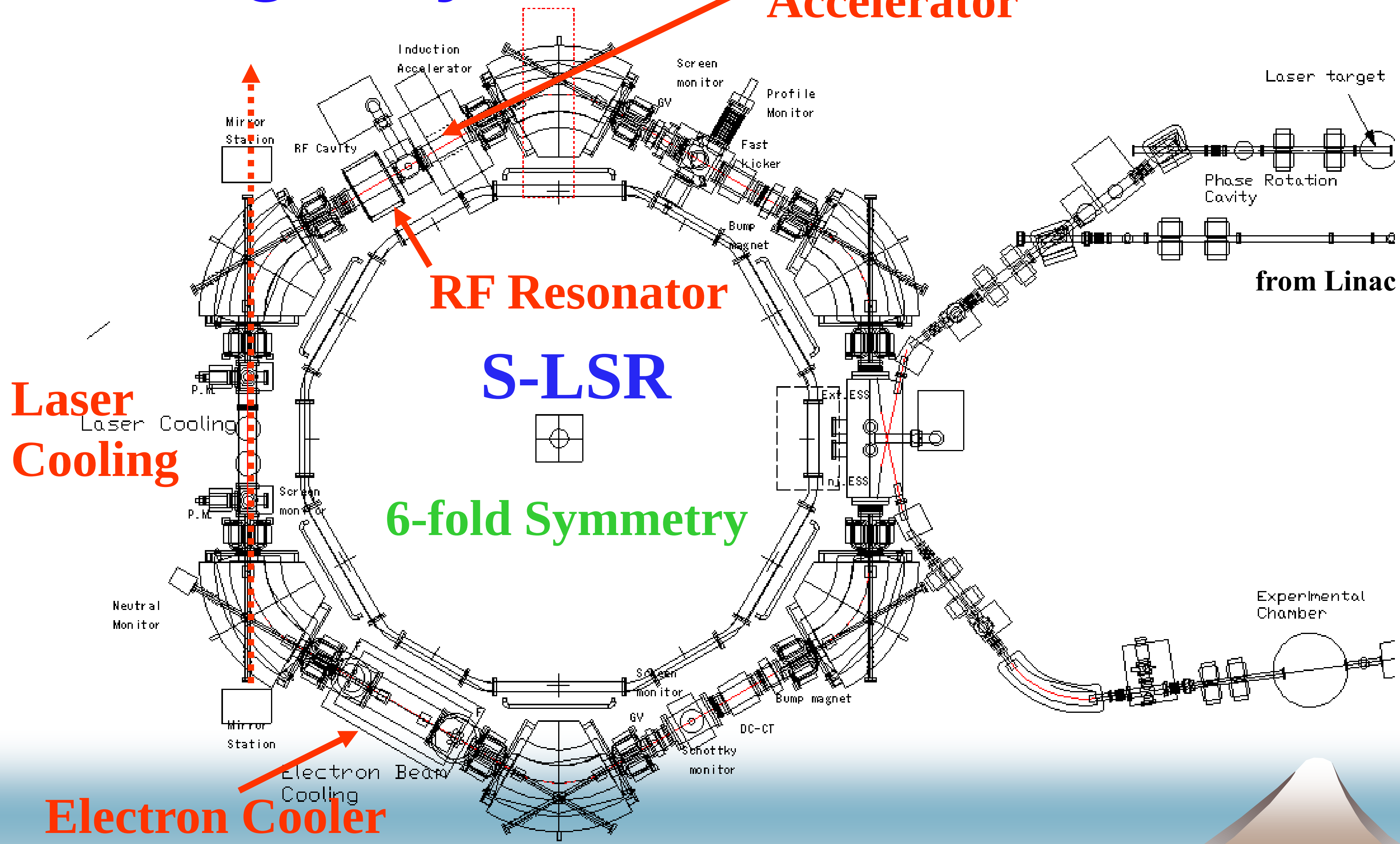

Induction Accelerator
RF Resonator
S-LSR
6-fold Symmetry
Laser Cooling
Electron Cooler
from Linac
Induction Accelerator
Mirror Station
RF Cavity
Screen monitor
Profile Monitor
Fast kicker
Bump magnet
Laser target
Phase Rotation Cavity
Laser Cooling
Ext.ESS
Inj.ESS
Neutral Monitor
Experimental Chamber
Electron Beam Cooling
DC-CT
Schottky monitor

Electron Cooler installed in S-LSR

Dr. Hicham Fadil

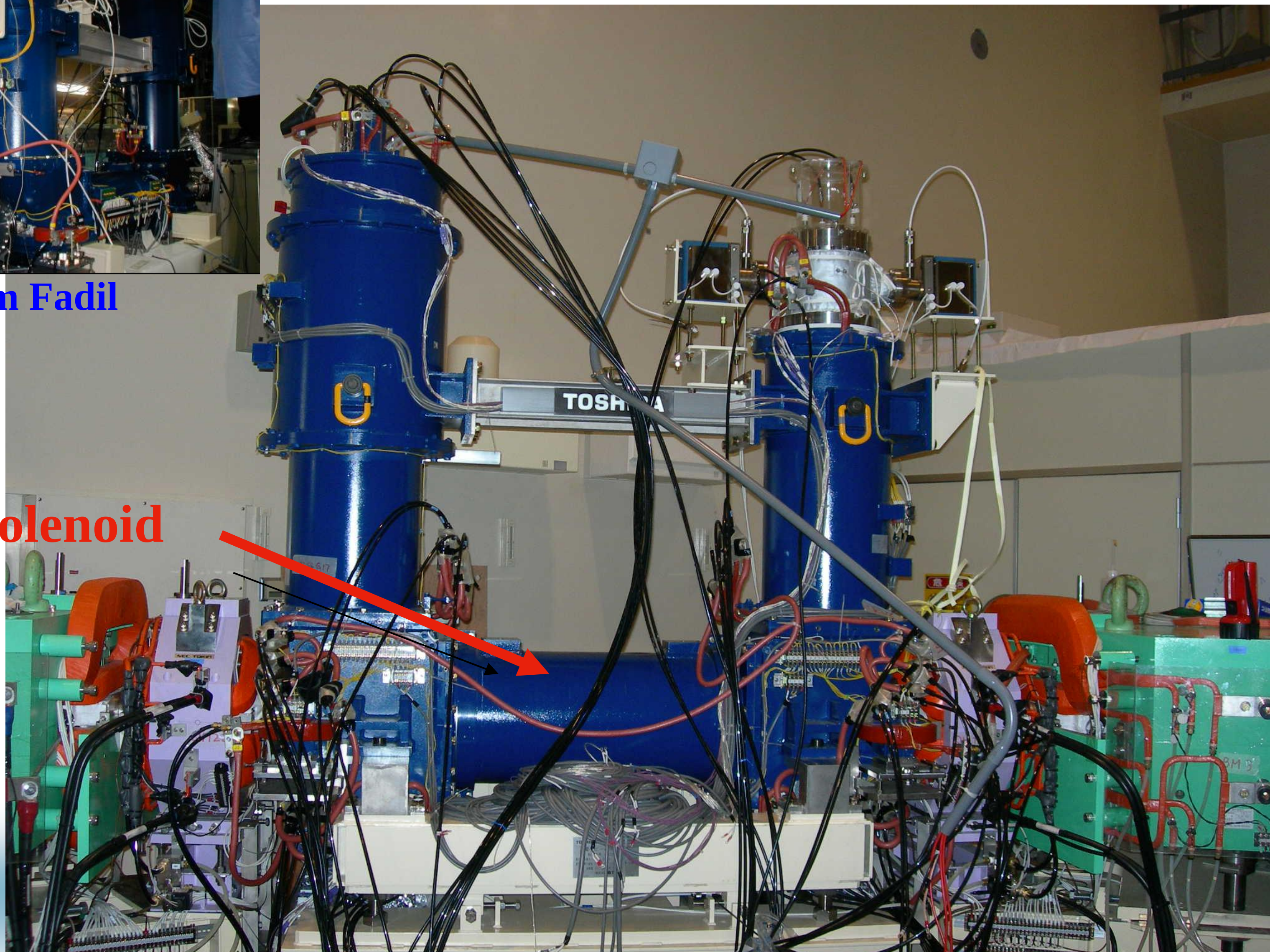

Phase Transition to 1D Ordered State

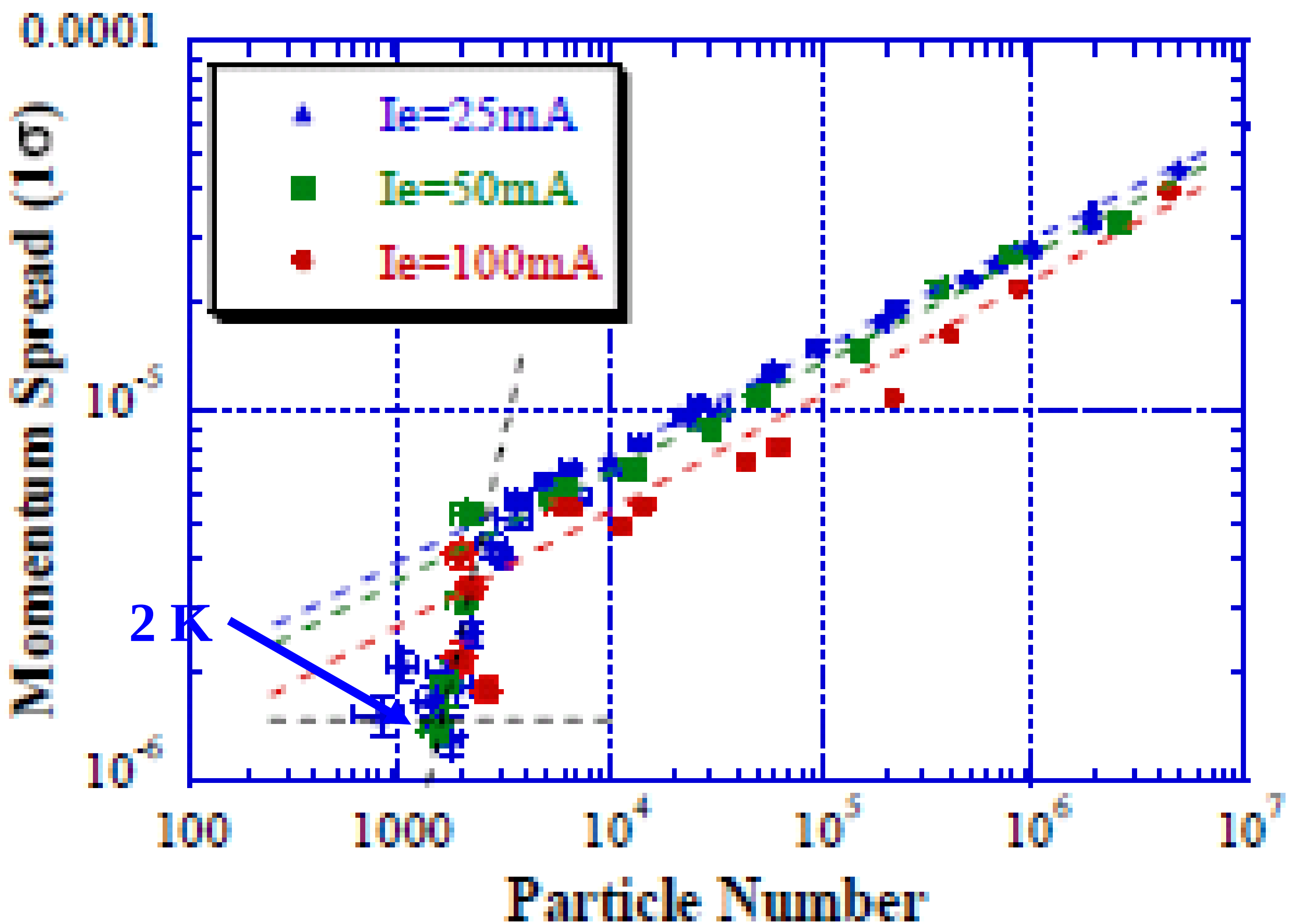

T. Shirai et al., PRL, 98 (2007) 204801

Simulation by H. Okamoto et al.

Expectation from Simulation

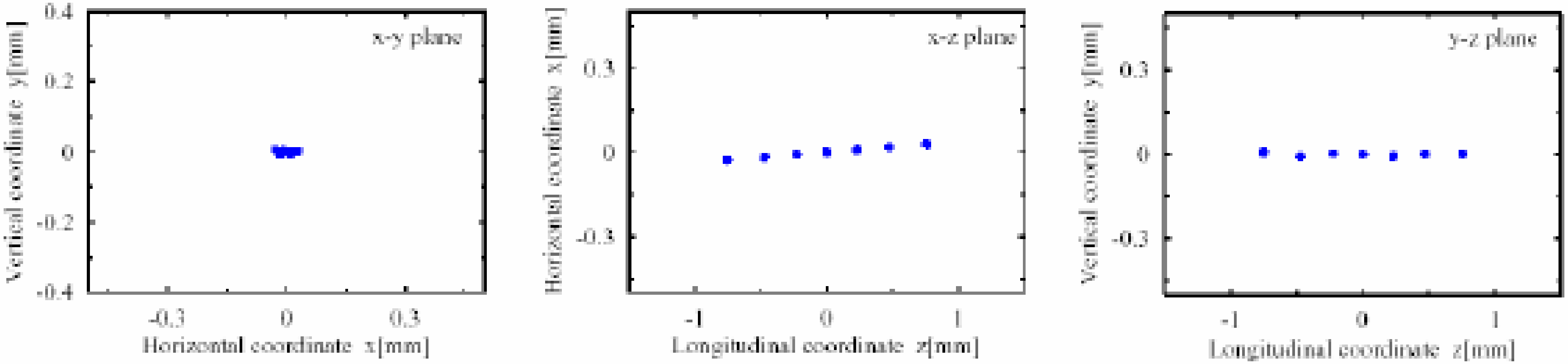

(a) 1 D String

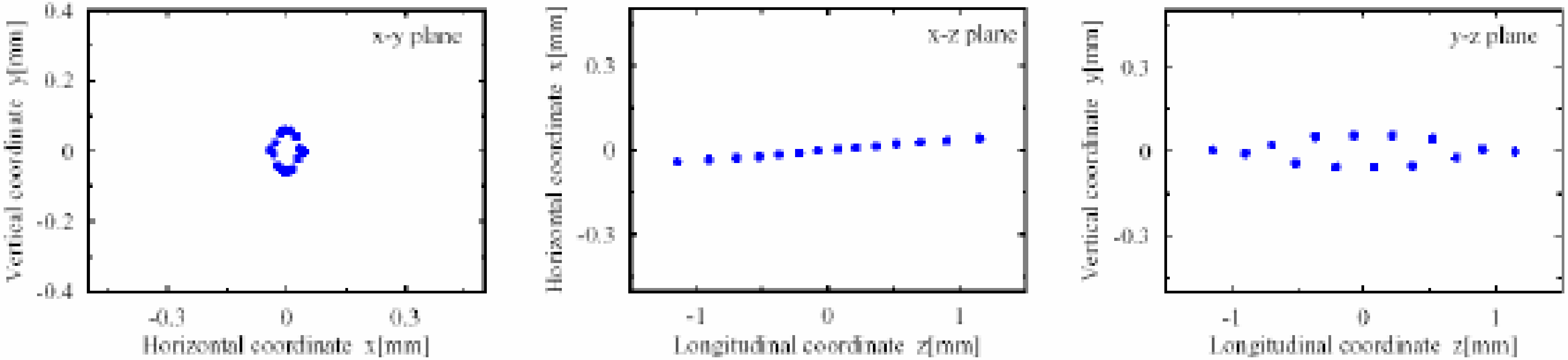

(b) 2D zigzag structure

Crystalline Beam in Circular RFQ, PALLAS

T. Schatz, U. Schramm, D. Habs:, Nature, 412, 717 (2001)

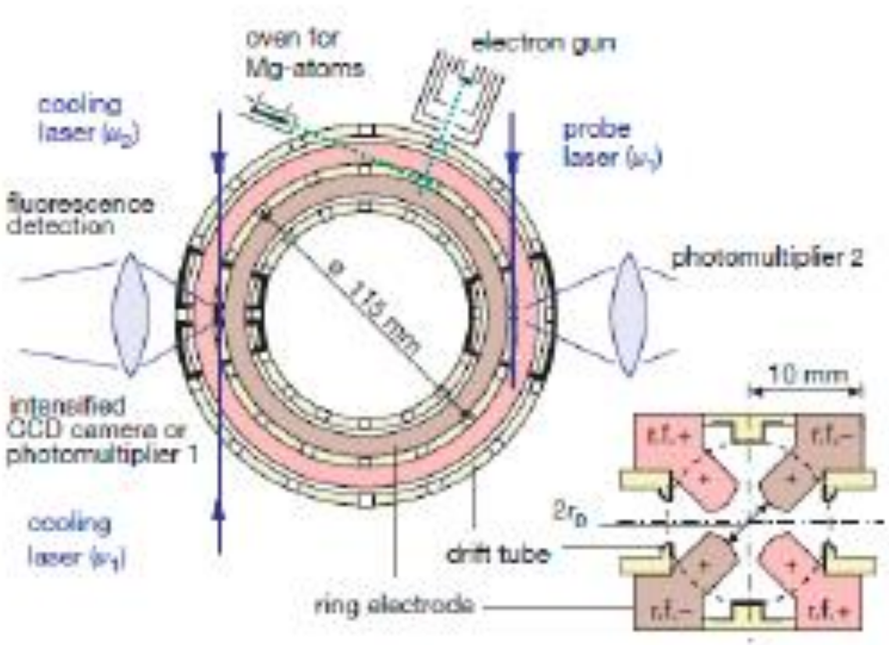

Structure of Circular RFQ, PALLAS

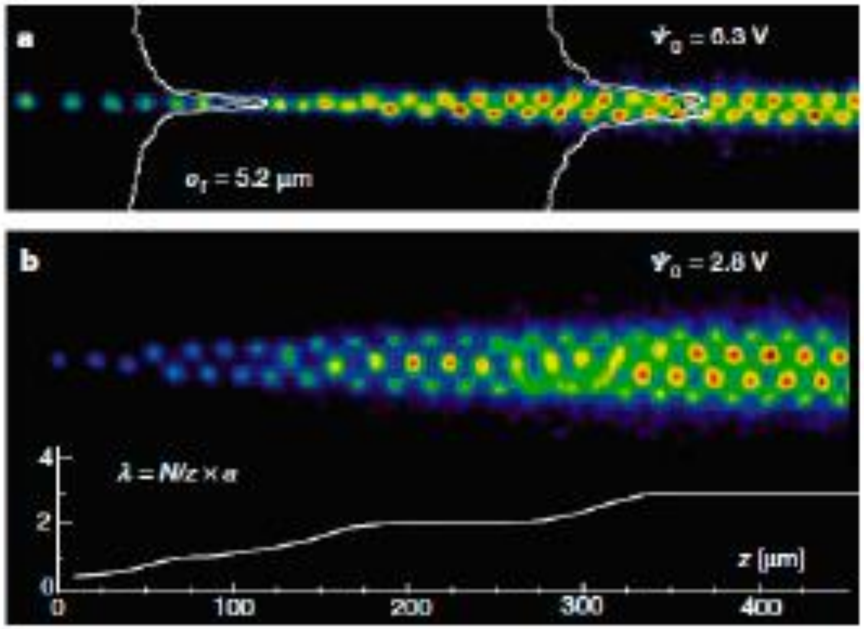

Images of ion crystals at rest in PALLAS

Excited States of Mg Ion

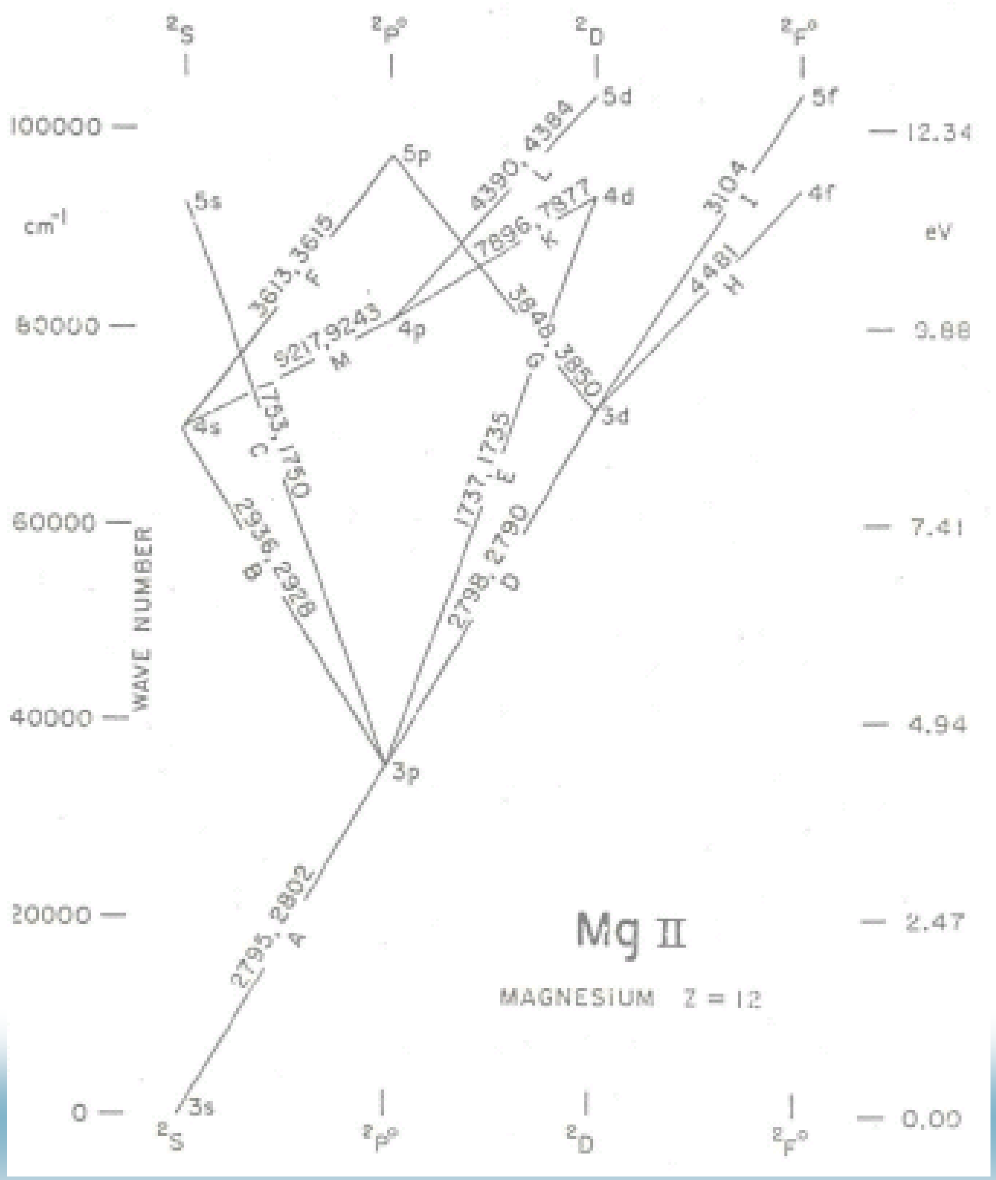

Principle of Laser Cooling (Longitudinal)

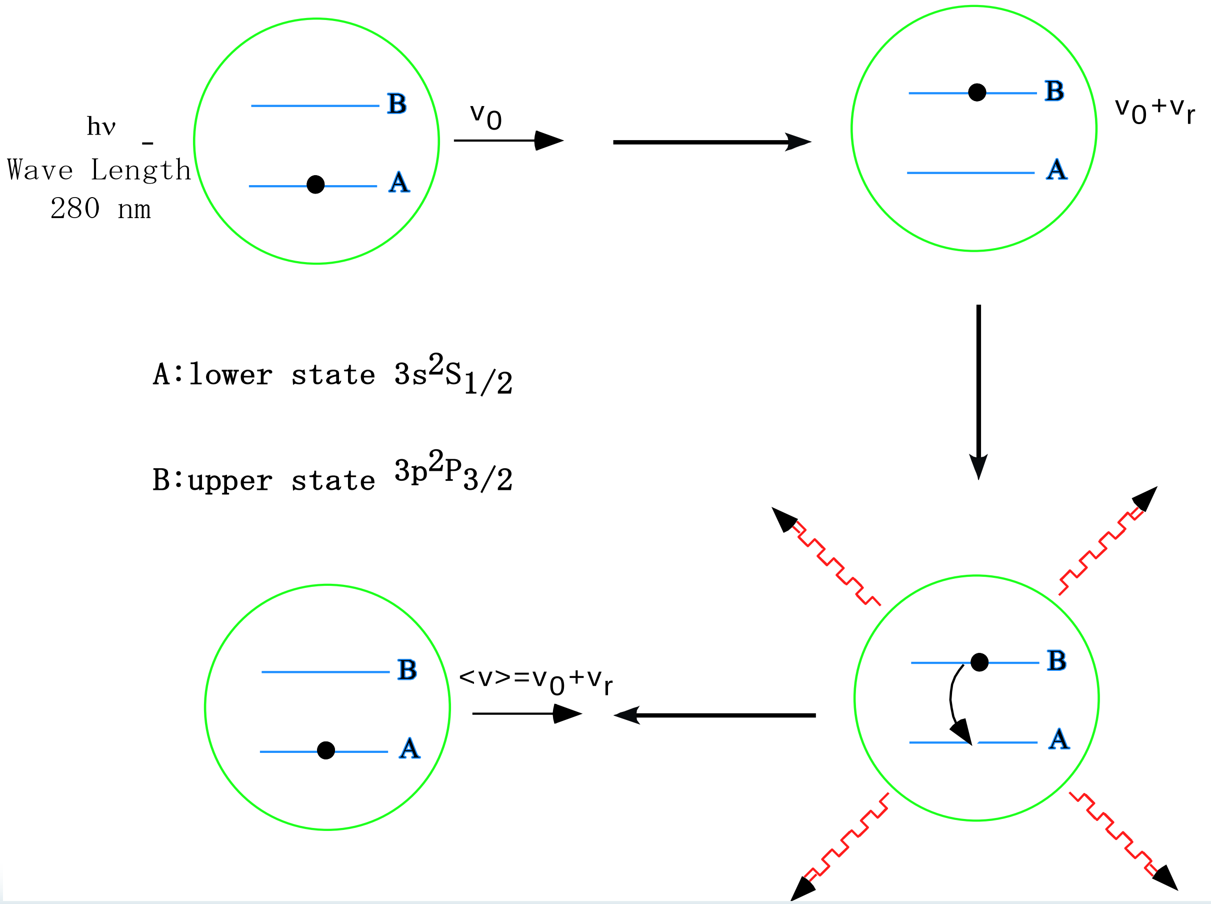

Block Diagram of Laser Cooling at S-LSR

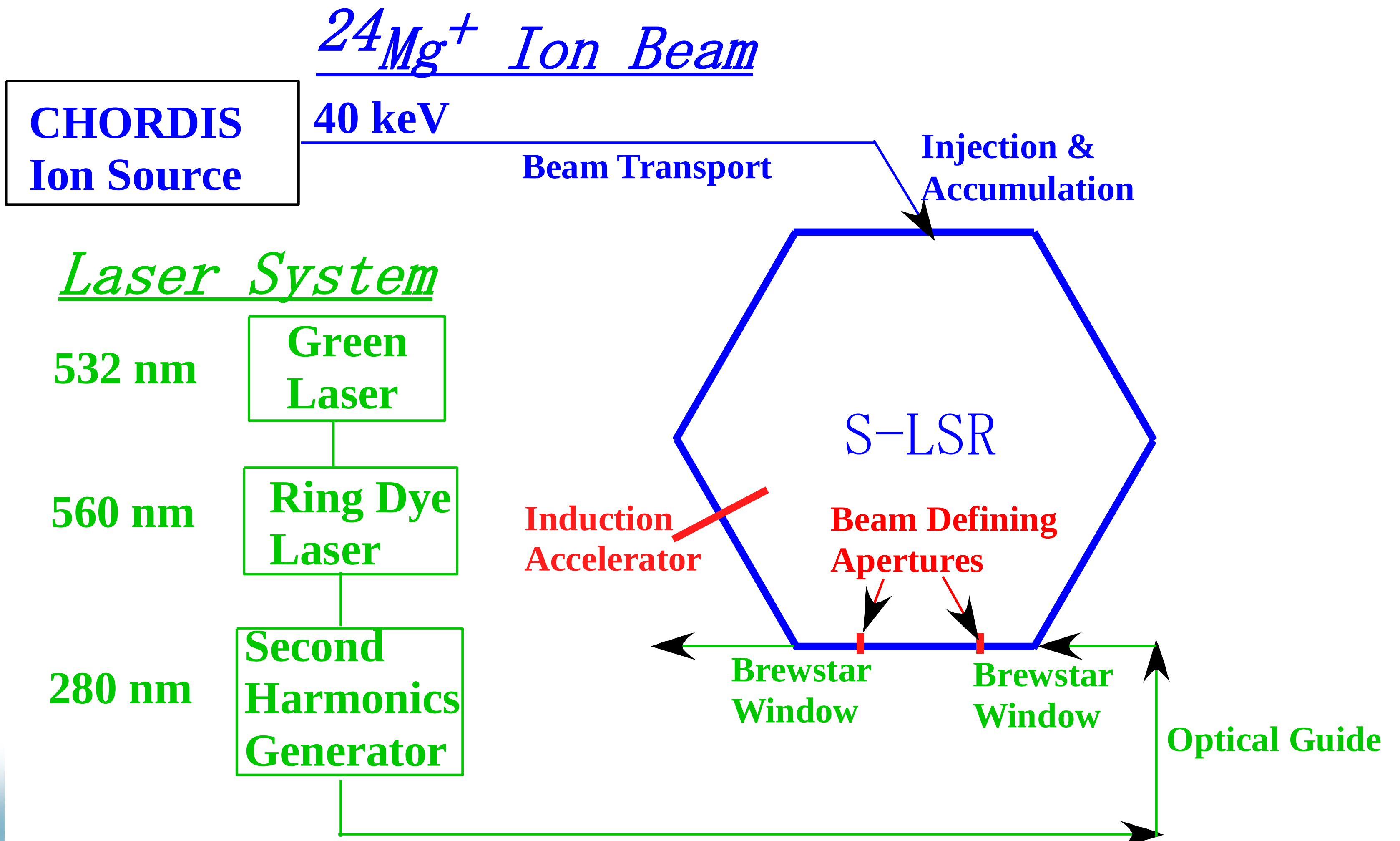

Observation of Transverse Beam Size by CCD Camera

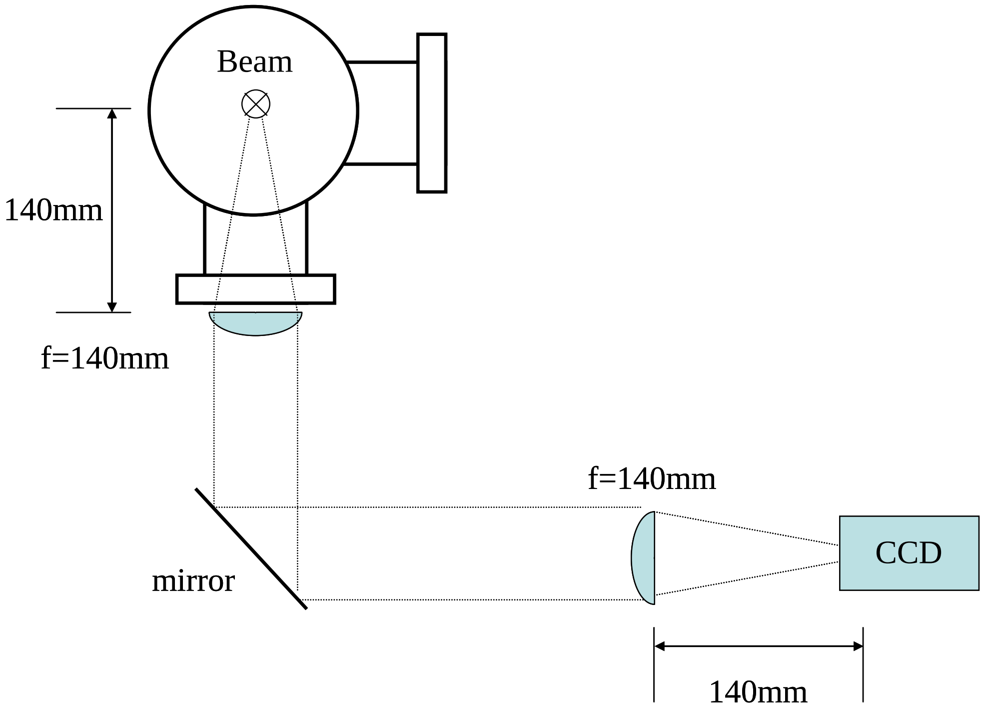

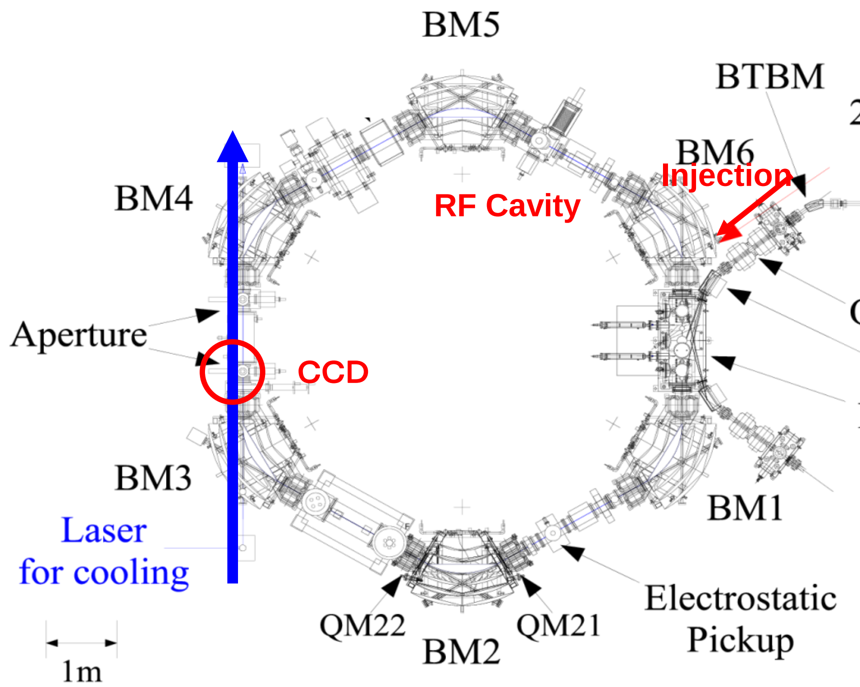

Cooled CCD Camera
(Hamamatsu Photonics C7190-11W)

Ion Observation with Emitted Light

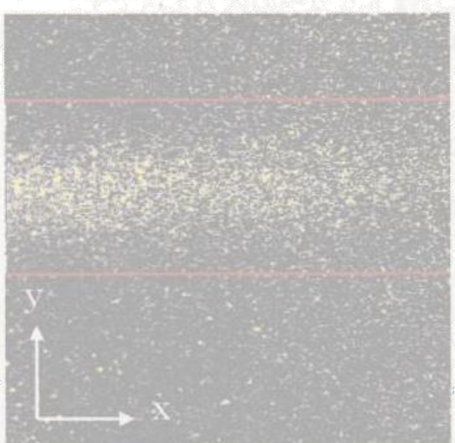

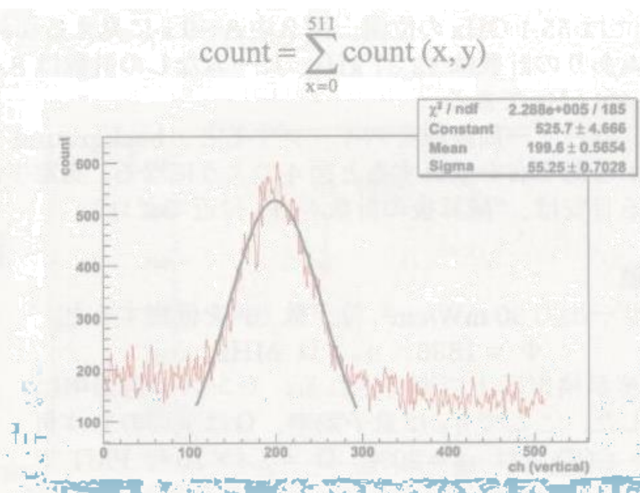

Laser Profile

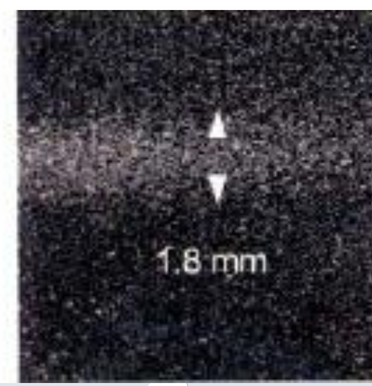

Fluorescent light from the ion beam

L-H Coupling

Only the relation:

$\nu_H - \nu_s$ = **integer**

is satisfied!

M. Nakao et al. Phys. Rev. ST Accel. Beams 15, 110102 (2012)

Transverse Laser Cooling by Synchro-Betatron Coupling

$(\nu_H, \nu_V) = (2.068, 1.105)$

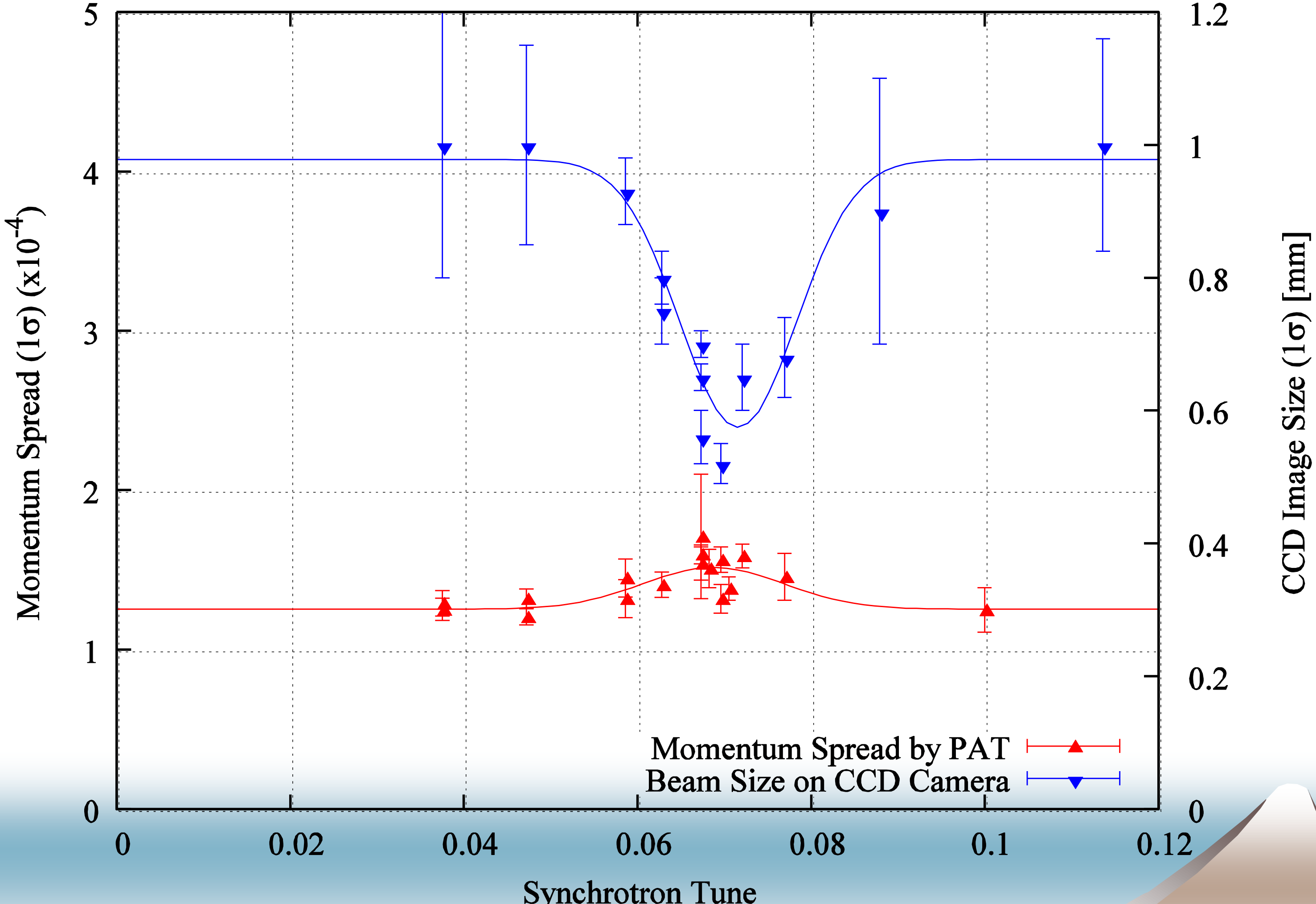

M. Nakao et al. Phys. Rev. ST Accel. Beams 15, 110102 (2012)

Time Variation of Transverse Beam Size for Various Synchrotron Tune

(Beam Intensity 1 x 10^7) **$(\nu_H, \nu_V) = (2.068, 1.105)$**

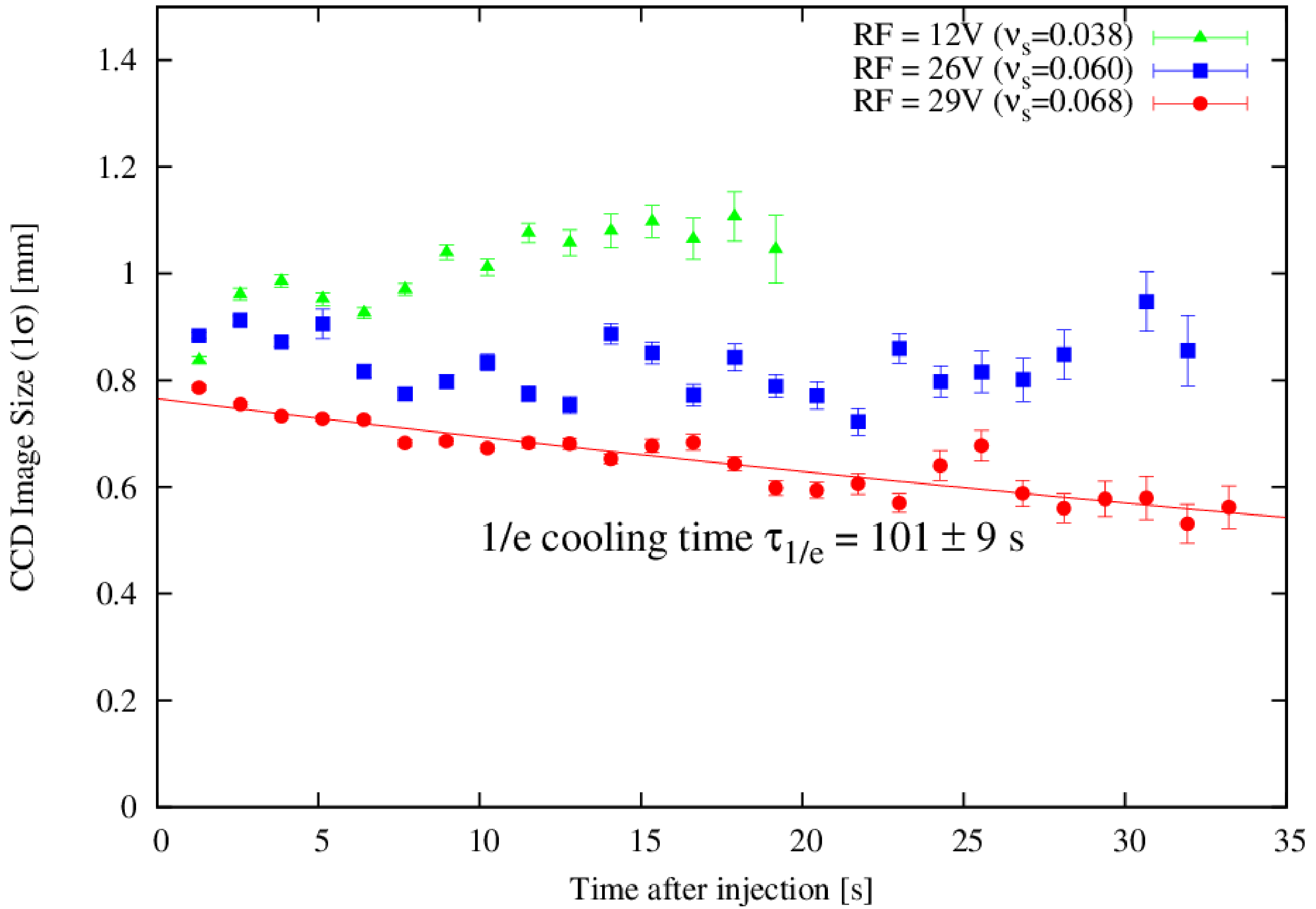

Controlled Scraping to Suppress IBS Effects

He Zhengqi et al., to be published

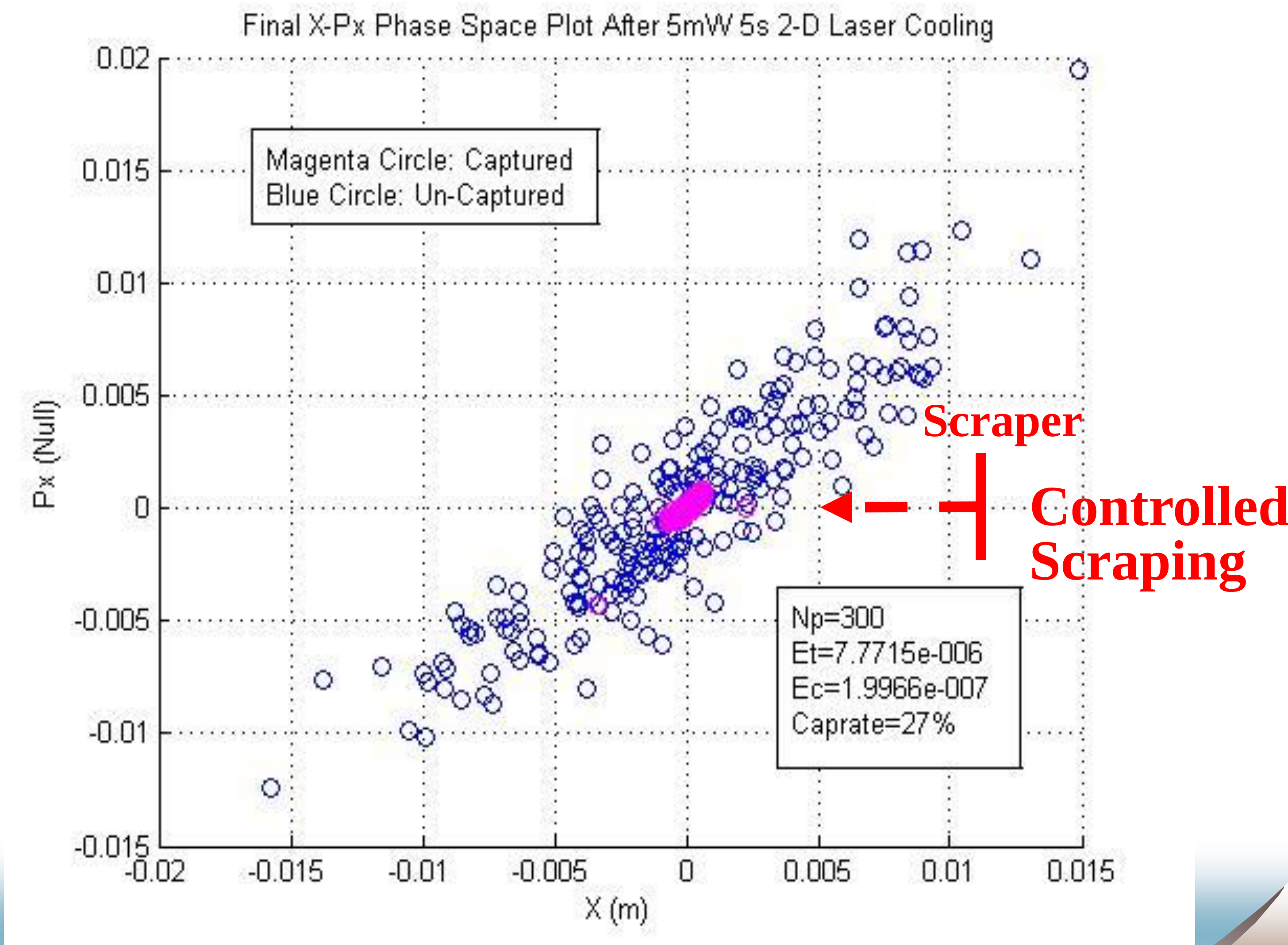

Scraping System for Intensity Reduction and Beam Size Measurement

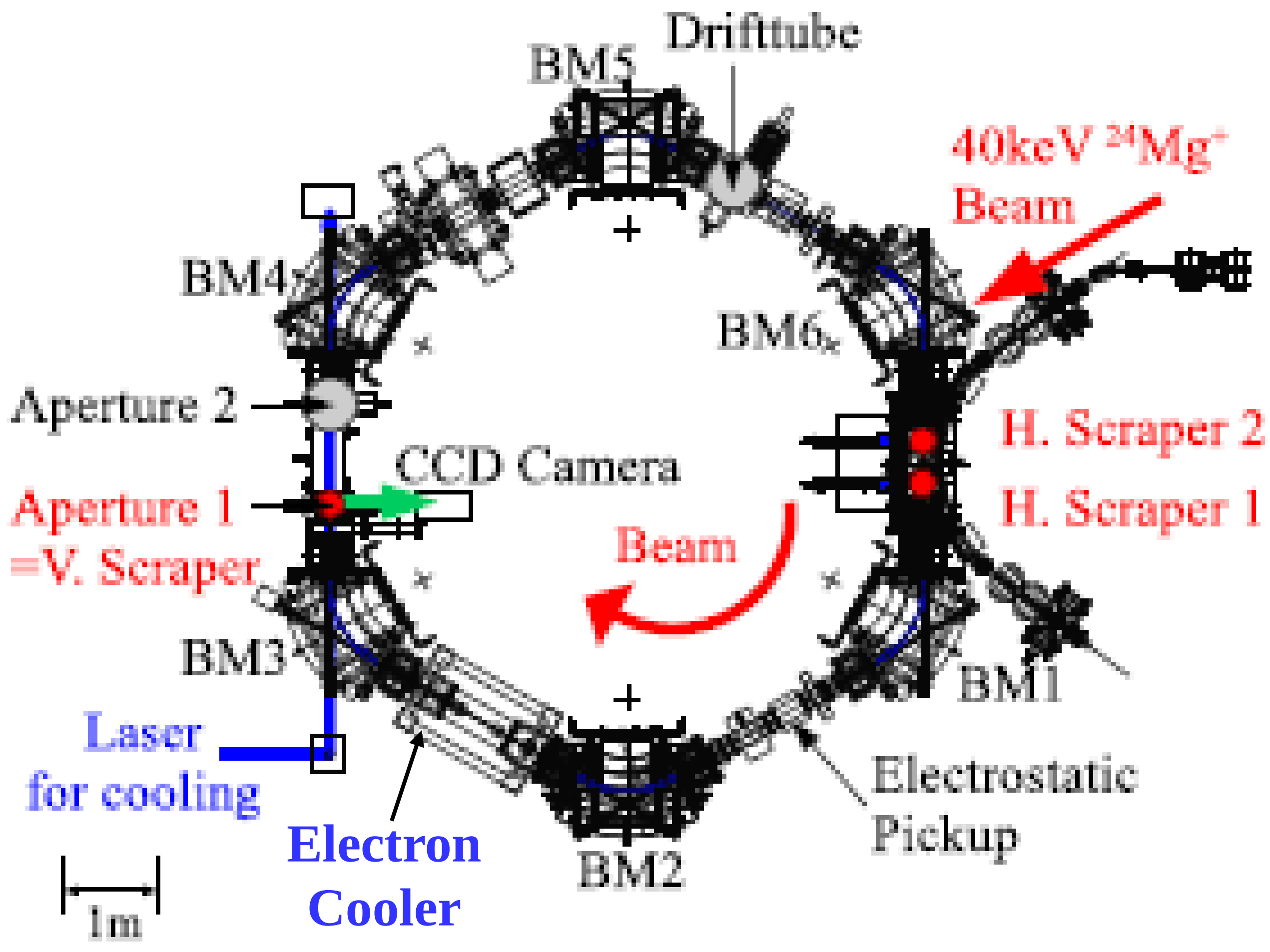

Beam Distribution Measured by Scraping

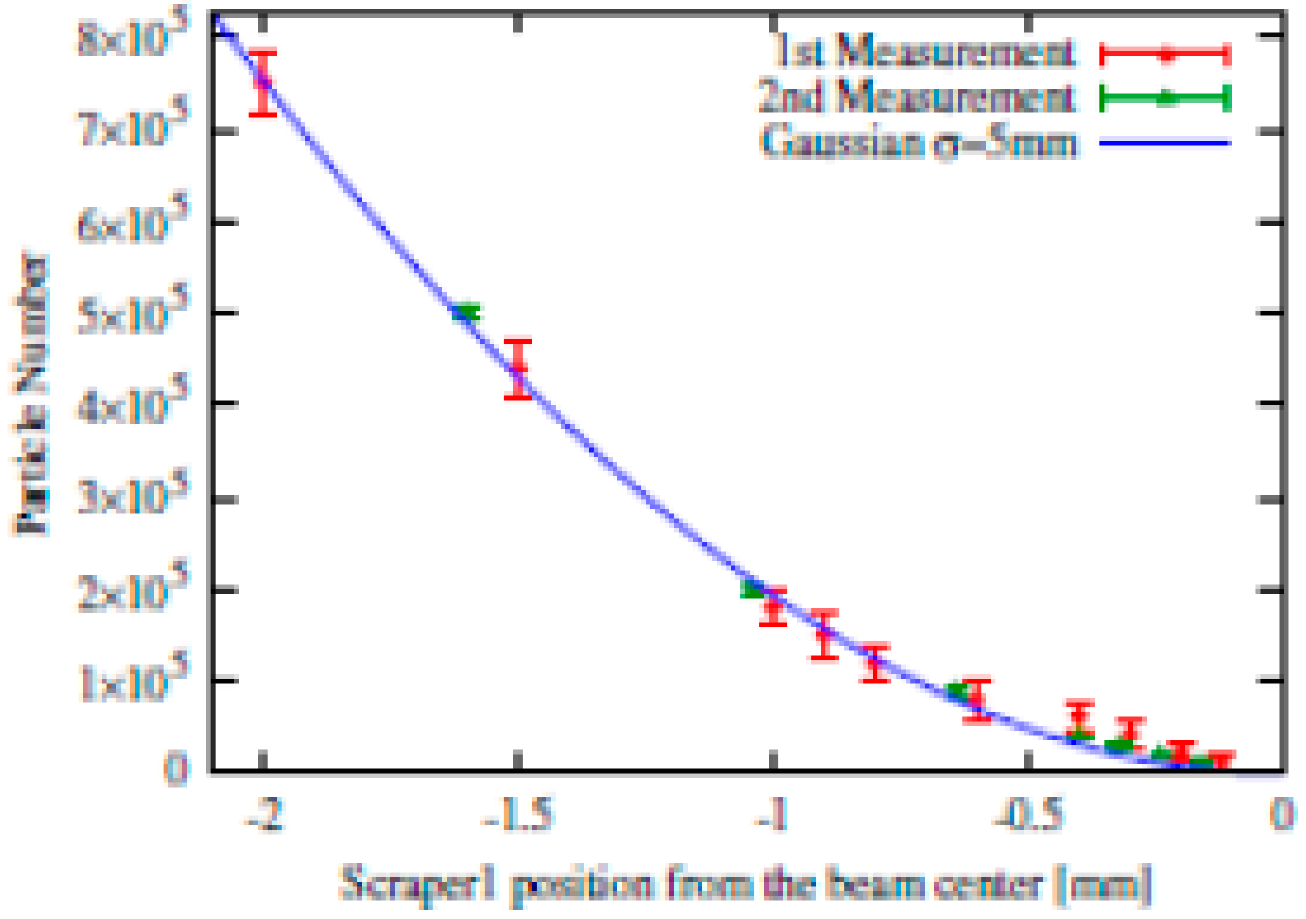

Efficiency Increase of Indirect Transverse Laser Cooling

H. Souda et al., Jpn. J. Appl. Phys. 52 (2013) 030202

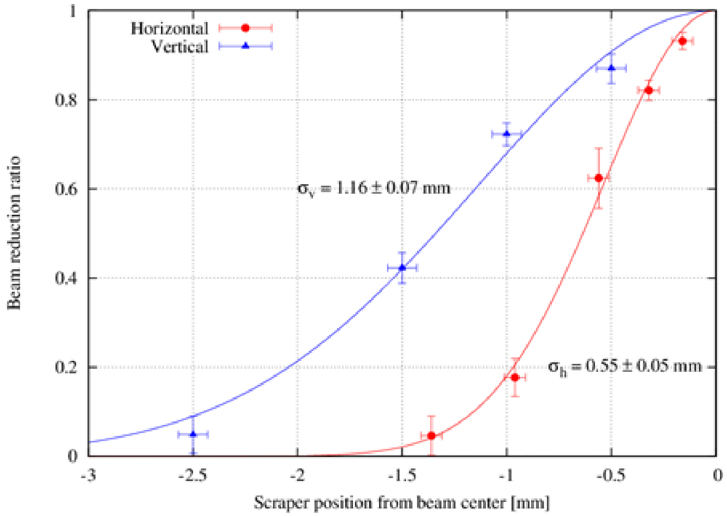

Beam size measurement by scraping

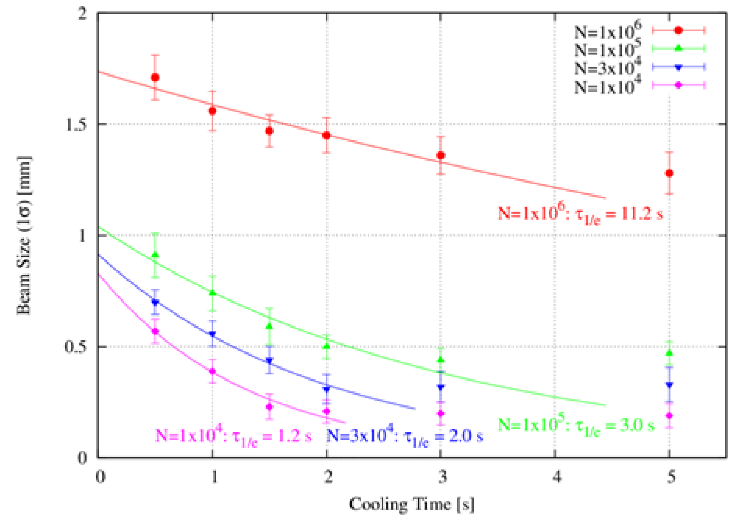

Time dependence of the cooled beam size

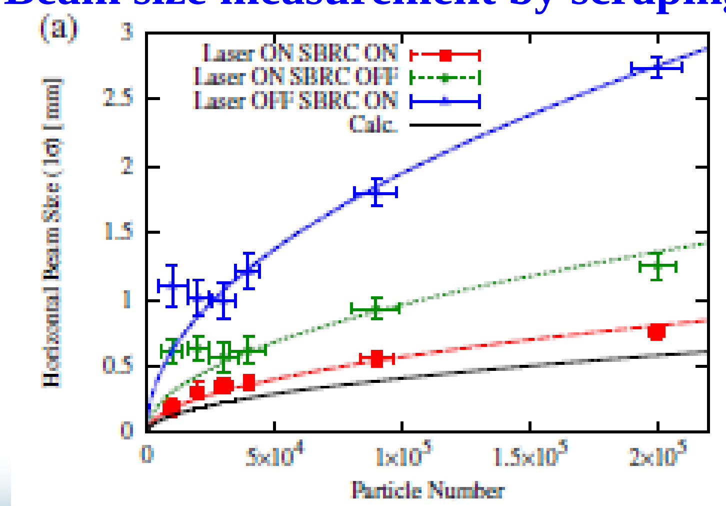

Horizontal beam size

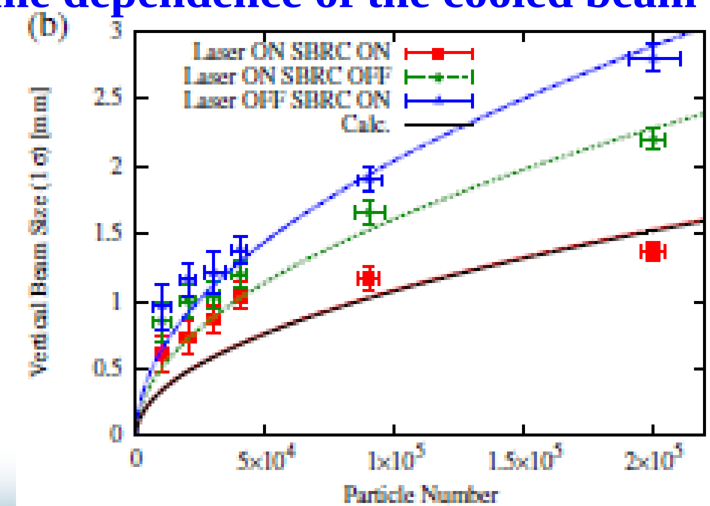

Vertical beam size

Ion Number Dependence of the Indirectly laser-cooled Laser cooled Beam Size

H-V Coupling is added

Relations:

$$\nu_H - \nu_s = \text{integer},$$

$$\nu_H - \nu_V = \text{integer}$$

are satisfied together with the use of a Solenoid

Comparison of Beam Sizes between 2D and 3D Indirect Laser Cooling

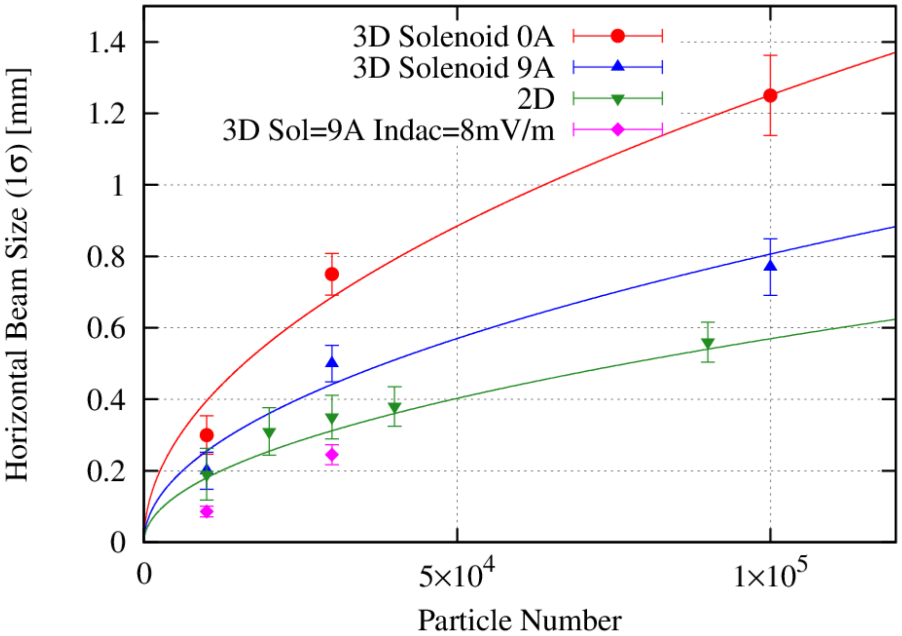

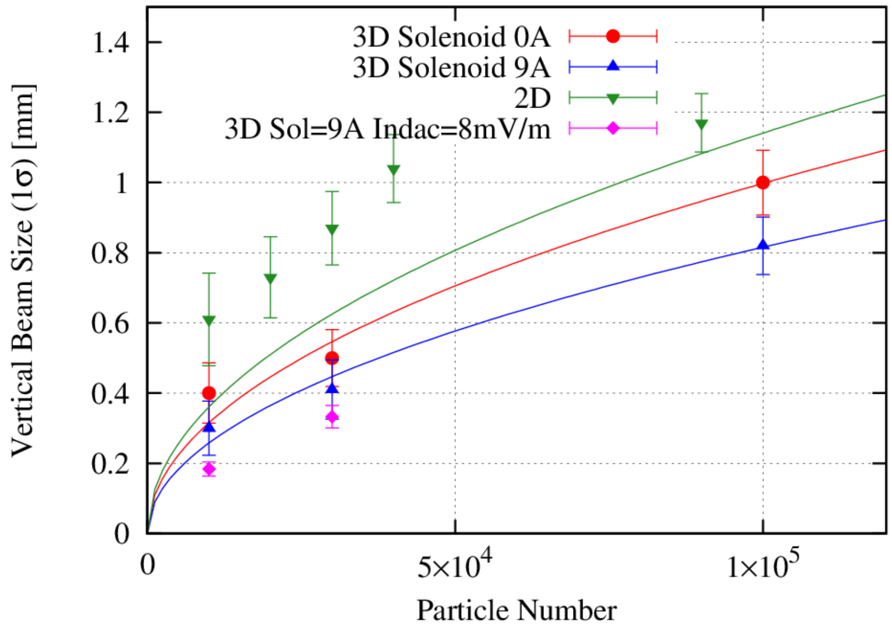

3D Laser Cooling + INDAC→Detuning Optimization

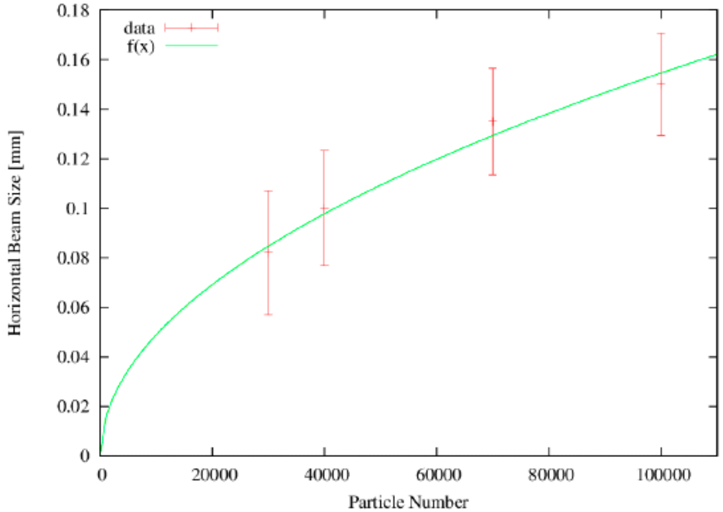

Horizontal Beam Size measured by CCD
0.08mm with the intensity of 3x10^4

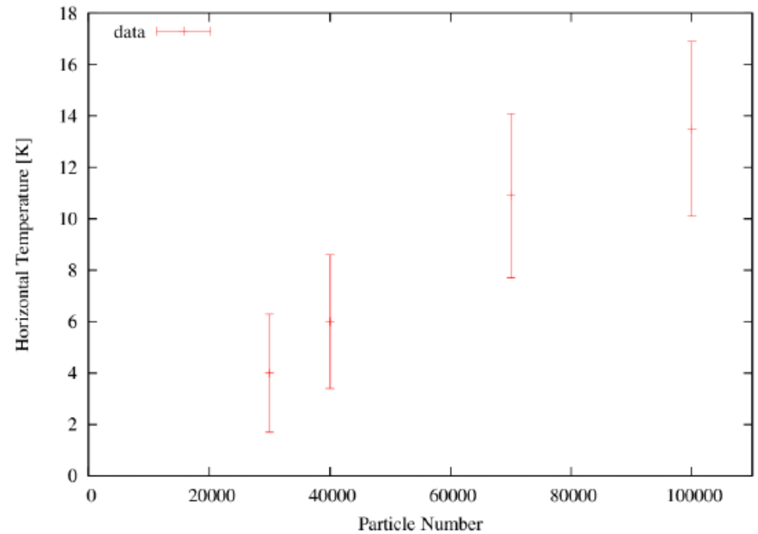

Horizontal Beam Temperature 7.0K with 3x10^4

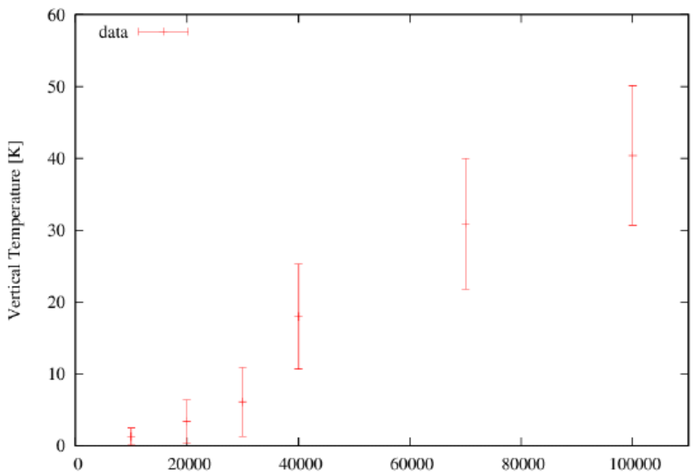

Vertical Beam Size measured by a Scraper
0.13mm with the intensity of 1x10^4

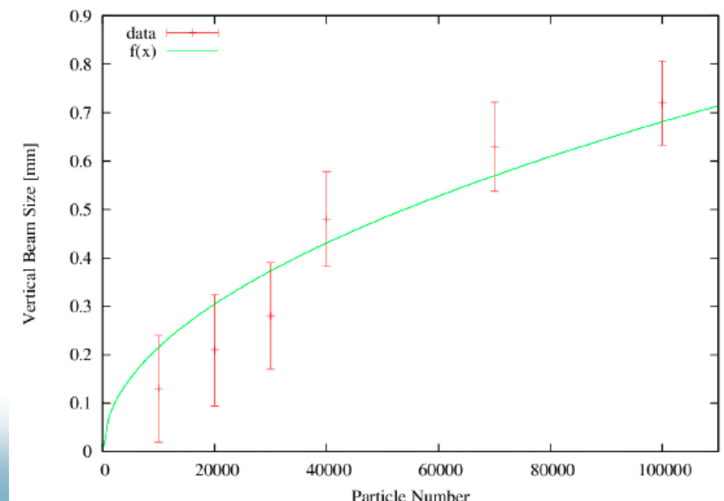

Vertical Beam Temperature 2.1K with 1x10^4

Comparison with Former Data

Year Ring	Method	Ion	Kinetic Energy	Intensity	$T_{//}$	T_H	T_V
1996 TSR	IBS	$^{9}Be^{+}$	7.3 MeV	2.0×10^{7}	15	4000	500
1998 TSR	Dispersive cooling	$^{9}Be^{+}$	7.3 MeV	1.0×10^{7}	few tens	~500#	~150 #
1999 ASTRID	IBS	$^{24}Mg^{+}$	100 keV	7×10^{6}	2-5	17	21
2001 PALLAS	RFQ	$^{24}Mg^{+}$	1 eV	1.8×10^{4}	<3 m	$T_{\perp}$<0.4	
2008 S-LSR	IBS	$^{24}Mg^{+}$	40 keV	1.0×10^{7}	11	-	500
2009 S-LSR	W SBRC (2D)	$^{24}Mg^{+}$	40 keV	1.0×10^{7}	27	$220^{\$}$	
2009 S-LSR	WO SBRC	$^{24}Mg^{+}$	40 keV	1.0×10^{7}	16		
2012 S-LSR	W SBRC (2D)	$^{24}Mg^{+}$	40 keV	1×10^{4}	(0.4)	20	29
2013.2.1 S-LSR	W SBRC (3D)	$^{24}Mg^{+}$	40 keV	1×10^{4}	-	40	11
2013.3.7 S-LSR (Δf=-190 MHz)	W SBRC (3D) (INDAC ON)	$^{24}Mg^{+}$	40 keV	1×10^{4}	-	8.1	4.1
2013.3.22 S-LSR (Δf=-26 MHz)	W SBRC (3D) (INDAC ON)	$^{24}Mg^{+}$	40 keV	1×10^{4}	-	7.0 (3×10^{4})	2.1

Controlled Scraping to Suppress IBS Effects

By M. Bussmann U. Schramm and D. Habs et al., SPARC07

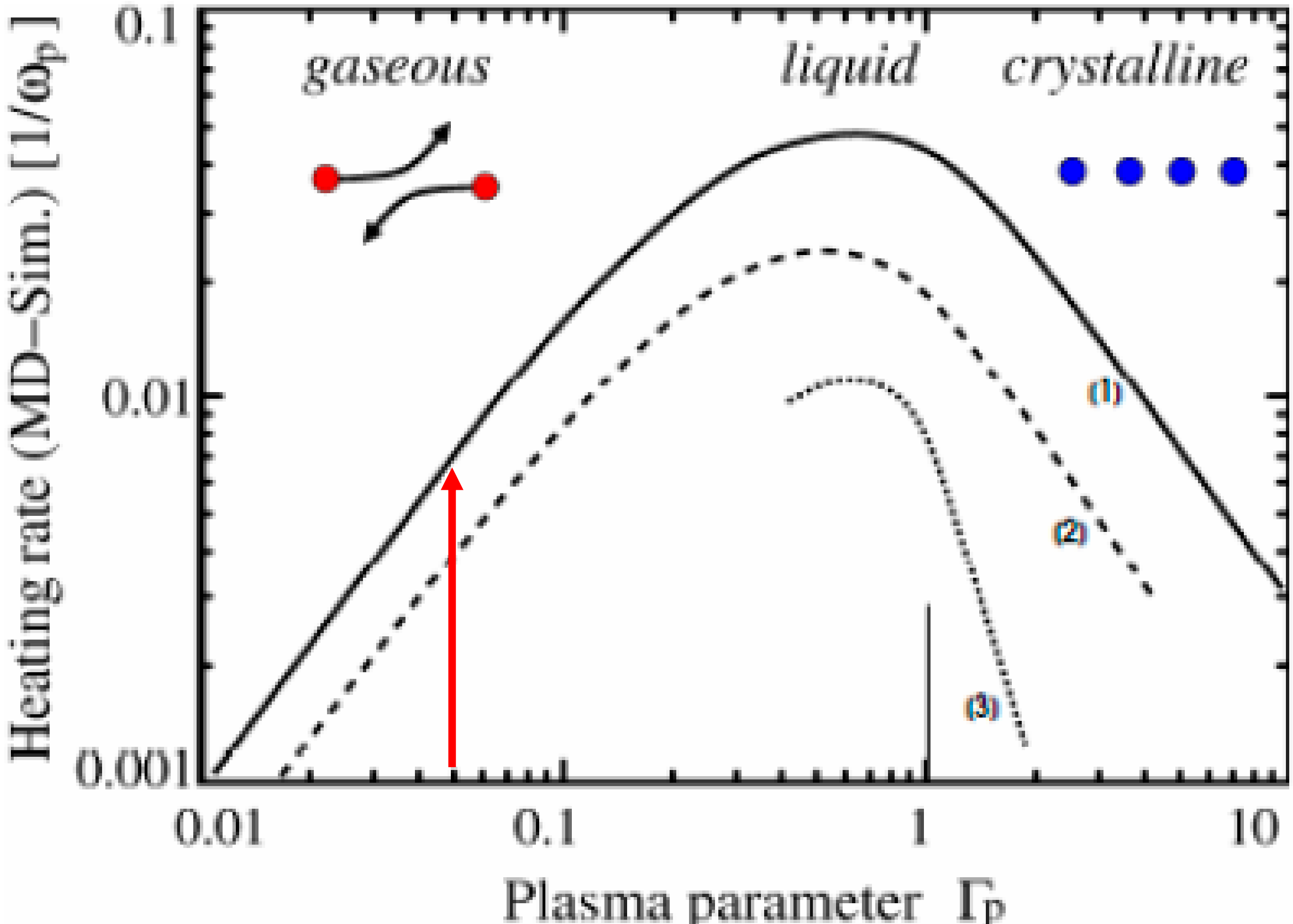

$$\Gamma_P = \frac{E_{Coulomb}}{E_{thermal}} = \frac{Z_{ion}^2 e^2}{4\pi\varepsilon_0 a_{WS} \cdot k_B T_{ion}}, \quad a_{WS} = \left(\frac{4}{3}\pi n_{ion}\right)^{-\frac{1}{3}}$$

(1): Q. Spreiter et al., NIM A 364 (1995), 239
(2): linear ion density reduced by a factor of 10
(3): string, J. Wei et al., PRL 80 (1998), 2606

MD Simulation

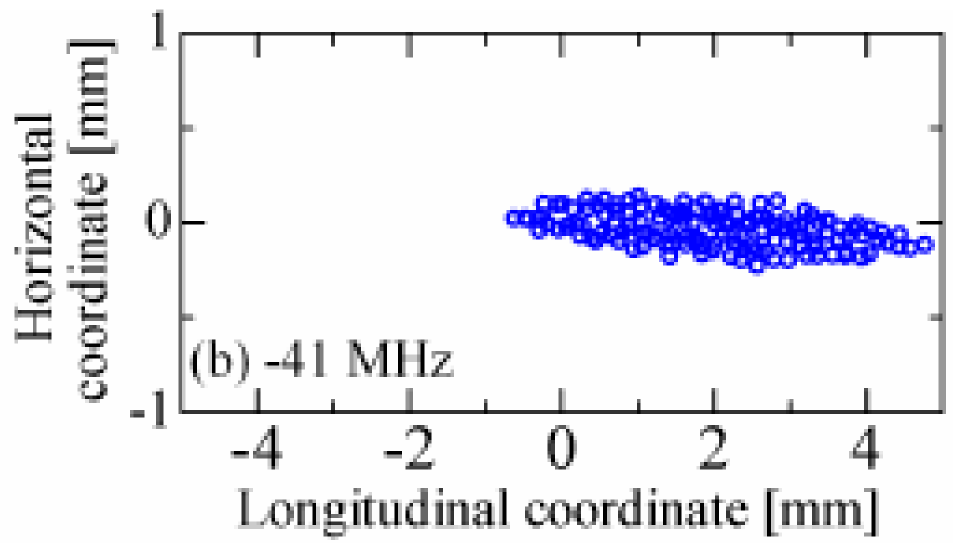

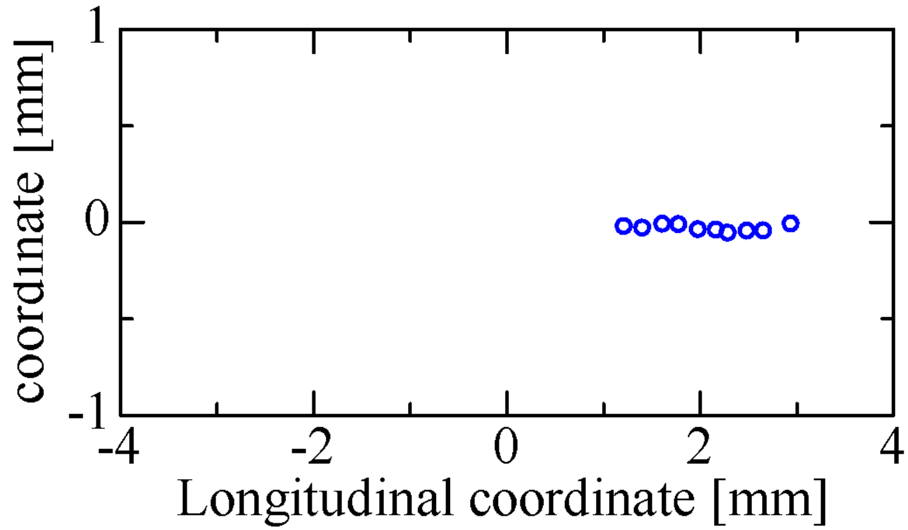

N = 10^4, detuning is -41 MHz
Laser Power is 8 mW

Experimentally attained!!
T_H= 7.0 K, T_V = 2.1 K

N = 10^3, detuning is -41 MHz
Laser Power is 8 mW

↓

1 D Crystalline string の形成

S-LSR リング　ラティスの特長

Shear Heating and Dispersion Suppressor

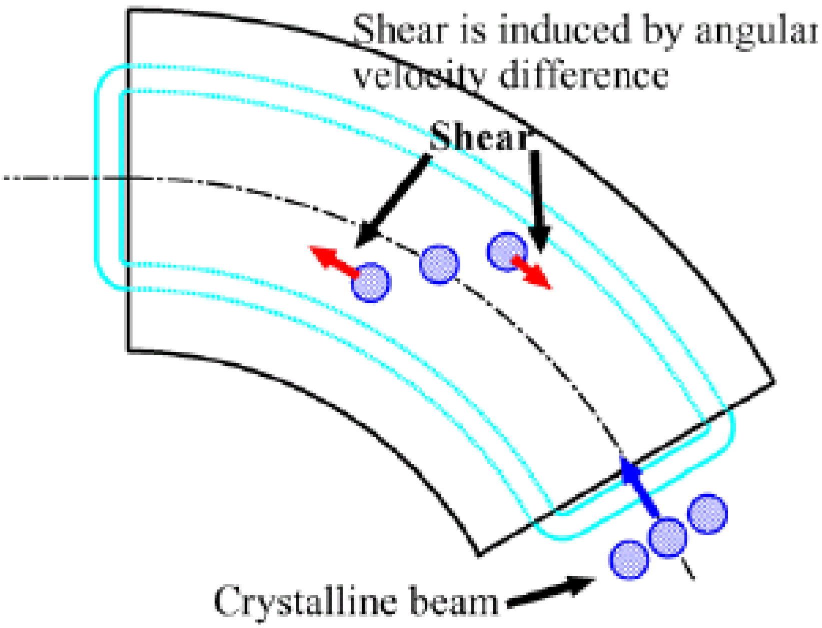

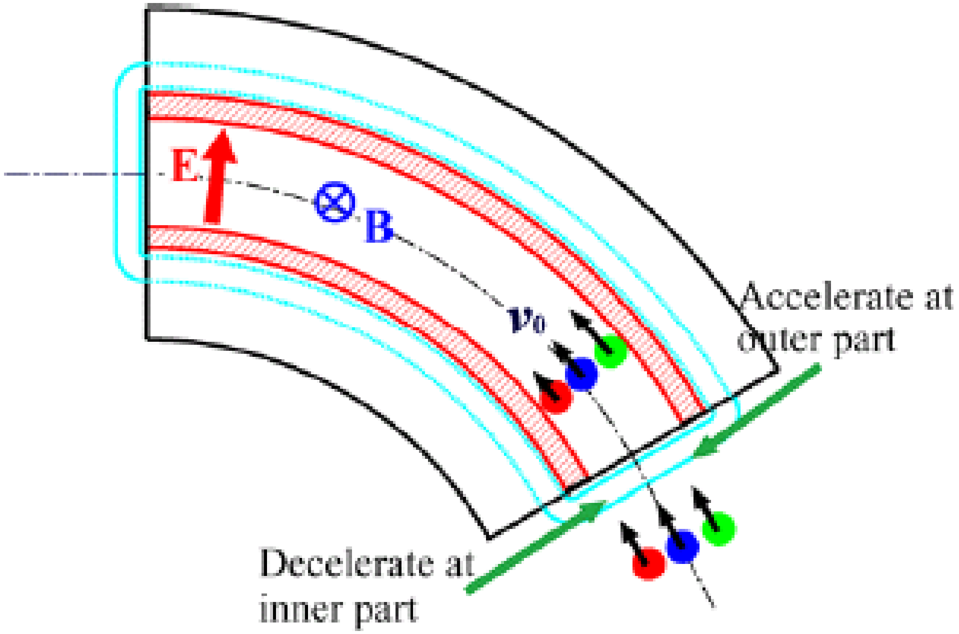

Dispersion Suppressor

$$\frac{d^2x}{ds^2}+\frac{3-n}{\rho^2}x=\frac{1}{\rho}\frac{\Delta W}{W}$$

Electric Field

$$\frac{d^2x}{ds^2}+\frac{1-n}{\rho^2}=\frac{1}{\rho}\frac{\Delta p}{p}$$

Magnetic Field

$$\frac{\Delta W}{W}=2\frac{\Delta P}{P}$$

Non-relativistic Case

↓

$$2\vec{E}=-(\vec{v}\times\vec{B})$$

Vacuum Chamber in the Magnet Section (includes the Electrodes)

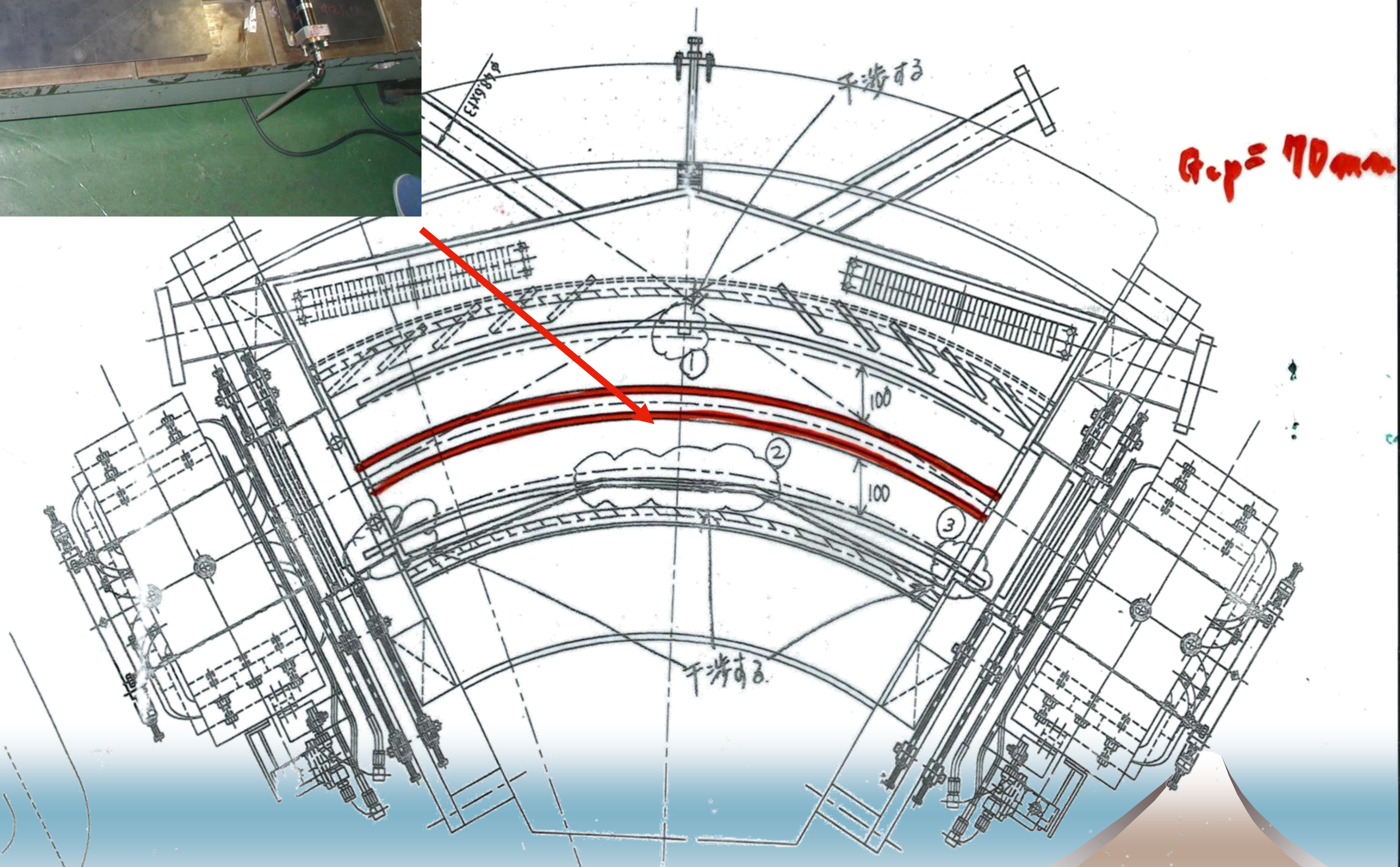

まとめと今後への提言(個人的願望)

1. SBRCによる3次元間接的レーザー冷却の実験的検証の実現
2. ビームスクレーピングによるIBS抑制を通じた冷却効率の改善
3. ビーム結晶化には更なる冷却力の強化が必要
   →レーザーの数、パワーの増強
   →スクレーピングによるビーム強度の更なる減少（あと一桁）に耐えるビーム検出効率の向上
4. **Dispersion Suppressed Lattice**を活用した3次元結晶化ビームの実現

謝辞

御清聴に感謝いたします。

本研究は文部科学省の「先進小型加速器のための要素技術の開発事業」及び京都大学グローバルCOEプログラム「普遍性と創発性から紡ぐ次世代物理学」の支援を得て行われました。